Characterization of rigid rod poly(pyridinium salt)s by conformational analysis, molecular dynamics, and steady-state and time resolved fluorescence

Michael P. Makowski* and Wayne L. Mattice†
Institute of Polymer Science, The University of Akron, Akron, OH 44325-3909, USA
(Received 24 March 1992; revised 9 July 1992)

Poly(4,4′-*p*-phenylene*bis*[2,6-diphenyl]pyridinium-*alt*-*bis*paraphenylene ditetrafluoroborate) and a model compound exhibit fluorescence emission from dilute solutions in dimethylformamide and vitrified samples dispersed in glassy poly(methyl methacrylate). The excitation and emission spectra, excitation polarization spectra and quantum yields for fluorescence were characterized in the dilute solution limit in dimethylformamide. Strong depolarization of the fluorescence was observed in dilute solution. The time-dependent decays of the intensity of the fluorescence were analysed to determine the lifetimes of the singlet excitation. In order to assist in the interpretation of the experiments, the conformations and molecular dynamics were investigated for an isolated dimer in the electronic ground state. The minimum energy conformations were found to be similar to those populated by other *ortho*-phenyl substituted *para*-phenylene structures in the solid state. The molecule experiences frequent transitions between rotational isomers that involve changes in dihedral angles in the main chain and between the main chain and pendant phenyl groups. The trajectory shows that there are correlations in these conformational transitions. The depolarization is attributed to an intramolecular non-radiative energy transfer mechanism coupled with frequent conformational changes in the main chain and pendant group torsional angles during the lifetime of the singlet excited state.

(Keywords: fluorescence; molecular dynamics; poly(pyridinium salt)s; rigid rod)

INTRODUCTION

Developments in rigid and semi-rigid backbone structures have been at the forefront of the effort to design new polymeric materials for specialized high performance applications. In 1989 Chuang and Harris reported the synthesis of a new rigid molecule of high molecular weight which has a backbone structure very near that of poly(phenylene)[1]. Derived from a clever mechanism reported by Katrinsky and Leahy for small molecule analogues[2], this family of polymers has an all-aromatic, *para*-linked backbone structure creating truly extended chain species, as depicted in *Figure 1*. Charges are incorporated into the backbone via regularly spaced quaternized aromatic nitrogen atoms, as a result of the novel 'ring transmutation' mechanism. The regularly spaced charges make these molecules much more soluble in common aprotic solvents than are the more conventional uncharged rigid rod polymers.

Here we report the steady-state and time resolved fluorescence of the polymer and model compound. A conformational analysis and molecular dynamics trajectory for the molecule in the electronic ground state are also presented, for assistance in the interpretation of the depolarization of the fluorescence. It is convenient to present first the absorption, excitation and emission spectra, and the fluorescence lifetimes. Finally, we report the anisotropy of the steady-state fluorescence, the conformational analysis and molecular dynamics, and the probable origin of the unusual behaviour of the anisotropy.

METHODS

Experimental

The model compound and two samples of the

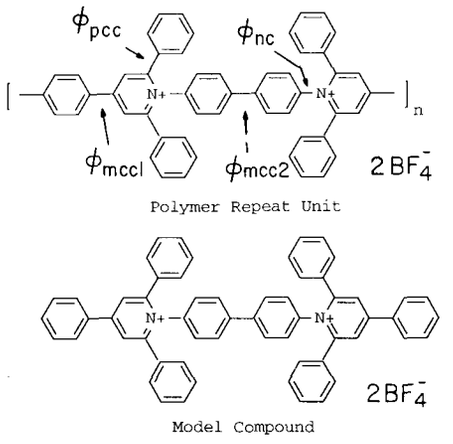

Figure 1 Non-hydrogen atoms in the model compound (bottom) and in the repeating structure of the polymer (top)

* Current address: NASA-Langley Research Center, Hampton, VA 23665-5225, USA
† To whom correspondence should be addressed

0032-3861/93/081606-07

polymer were kindly supplied by Professor Frank W. Harris. Molecular weights for the two samples of the polymer were estimated from zero shear intrinsic viscosities, measured at 30.0°C in dimethylformamide (DMF) in the presence of excess supporting electrolyte (0.098 N $LiBF_4$), using a 4-bulb Cannon–Ubbelohde shear dilution viscometer. The molar mass was correlated with the viscosities using a relationship derived by Abdel-Khalik and Bird for the flow of rod-like molecules under zero shear[3]:

$$[\eta]^0 = \left(\frac{Ll^3\pi}{20M}\right)\ln(l/d) \quad (1)$$

where L is Avogadro's number, M and l are the mass and length, respectively, of the rod, and (l/d) is the aspect ratio. The diameter and length per repeating unit were determined from energy minimized structures using Sybyl 5.4 (Tripos Associates, Inc., St Louis). The estimates of molecular weight were 20×10^3 and 50×10^3. Henceforth these two samples will be denoted by M20 and M50, respectively. Rigid molecules with these molecular weights have end-to-end distances of 40 and 120 nm, respectively. Their degrees of polymerization are 26 and 65.

Absorption spectra were measured at ambient temperature with a Hewlett–Packard 8451A diode array spectrophotometer. The samples were dissolved in spectrograde DMF supplied by either Aldrich or J. T. Baker. Excess supporting electrolyte was not used in these measurements.

Steady-state fluorescence was measured with an SLM 8000C spectrofluorometer. The light source was an ozone-free 450 W xenon arc lamp. Double grating excitation and single grating emission monochromaters were used, with slit widths of 8–16 nm. Unless specifically stated otherwise, right angle illumination using an enhanced sensitivity single cuvette sample accessory (SLM) was employed. Two 10 mm Glan–Thomson prisms were employed for polarizing the incident and emitted radiation for the anisotropy measurements. The anisotropy of the fluorescence was determined as[4]:

$$r = \left(\frac{I_{vv} - GI_{vh}}{I_{vv} + 2GI_{vh}}\right) \quad (2)$$

$$G = \frac{I_{hv}}{I_{hh}} \quad (3)$$

where I is the measured intensity, and v and h as subscripts denote vertical and horizontal polarization, respectively. The subscripts are listed in order of incident and emitted light, respectively. The samples in DMF had maximum optical densities of 0.1–0.2, corresponding to concentrations of 10^{-6}–10^{-7} M in repeat units. Fluorescence quantum yields were determined in DMF at ambient temperature, using the method of slopes[5] and quinine bisulfate monohydrate in 1.0 N H_2SO_4 as the standard[6]. A fluorescence quantum yield of 0.56 at 348 nm was assumed for the standard.

Steady-state fluorescence for samples dispersed in glasses of poly(methyl methacrylate) (PMMA) was measured with a 45° front face geometry using a slide holder accessory (SLM). Solutions of the model compound in distilled methyl methacrylate were prepared at approximately 10^{-6} M, yielding maximum optical densities of 0.1–0.2. Approximately 5 ml of the solution was introduced into the mould (25 ml Erlenmeyer flask or 10 ml test tube) and thermally polymerized, in the absence of initiator, using a temperature-controlled silicon oil bath. N_2 was bubbled through the solutions beforehand to minimize void formation and quenching of the radical chain ends by O_2. The solutions were heated to 75°C for 2 h, forming a prepolymer viscous fluid. The temperature was then gradually increased to 90°C and the polymerizations were left overnight (~10 h). The vitrified glass was retrieved by cooling and then breaking the mould with a hammer. The disc-like samples from the Erlenmeyer flasks were used for the steady-state measurements, and the cylindrical samples (~10 mm diameter) resulting from the test tubes were used for the time resolved work. No evidence of heterogeneity or bubble formation was seen in the samples or in the PMMA blanks, which were made in the same fashion.

Fluorescence lifetimes were measured using an instrument with a frequency doubled, mode locked 2 W Nd:YAG laser with a principal wavelength of 523 nm and a repetition rate of 76 MHz, a Rhodamine 6G ultra-fast dye laser and cavity dumper set for 3.8 MHz, all from Coherence Co. A single grating monochromater and microchannel phototube were used for photon detection. Right angle illumination with an excitation wavelength of 305 nm was used. A 399 nm cutoff filter was placed directly after the sample cell to reduce scattered light. Decay curves were stored in the range 0–1024 channels, with the time calibration set at 0.0487 ns/channel. Data were collected until ~10^5 counts were accumulated in the peak, with average acquisition times being 10–15 min. Freshly prepared solutions were used to minimize the influence of impurities arising from photoreaction[7]. The Raman peak from water (338 nm) was used to determine the laser pulse profile, which subsequently was used with a nonlinear least squares method to analyse the time resolved decay profiles.

Simulations

Energy minimizations and molecular dynamics trajectories were performed using Sybyl 5.4 (Tripos Associates, Inc., St Louis). All calculations were performed on the isolated chain in the absence of solvent and counterions. Energy minimizations were conducted using the Tripos force field, with and without electrostatic potentials. A semi-empirical Huckle molecular orbital calculation was used to determine partial charges and bond orders. Since steric effects far outway electronic effects insofar as the conformational properties of these molecules are concerned, we performed the subsequent analysis without inclusion of partial charges.

The total potential energy for the dimer species was minimized using a conjugate gradient method. The dynamics trajectory was then calculated by integrating the classical equations of motion for all non-hydrogen atoms at steps of 0.5 fs. The total trajectory has a length of 0.25 ns, but only the last half of the trajectory was used in the analysis. The trajectory that was analysed has a length equivalent to the fluorescence lifetime measured for the dimer in DMF. The simulation was carried out at a constant temperature of 300K, without rescaling of velocities. Data were collected every 25 fs, and the length of the trajectory was 0.25 ns. The analysis uses snapshots spaced at 100 fs over the last half of the trajectory.

RESULTS AND DISCUSSION

Absorption spectra

Figure 2 depicts the absorbance of M20 at ambient temperature in DMF. The model compound and M50 also exhibit broad spectra having single maxima at 320–350 nm, indicative of closely spaced π–π^* transitions common to aromatic species of this type. A similar molecule, 1,2,4,6-tetraphenylpyridinium perchlorate, exhibits nearly the same spectrum, with a maximum at 312 nm (ethanol, 293 K)[8]. The absorption bands in this family of *ortho*-substituted pyridinium salts have components of two electronic transitions associated with an intramolecular charge transfer complexation of the 2,6- and the 4-substituent with the heteroring, respectively[8]. Based on the spectral similarities to other phenyl-substituted pyridinium salts[8,9], the absorption bands of the polymers and model compound in this study arise from the same electronic transitions as those in the molecules studied previously. Molar extinction coefficients and absorption maxima are listed in *Table 1*. The absorption maxima shift to lower energies with increasing molecular weight.

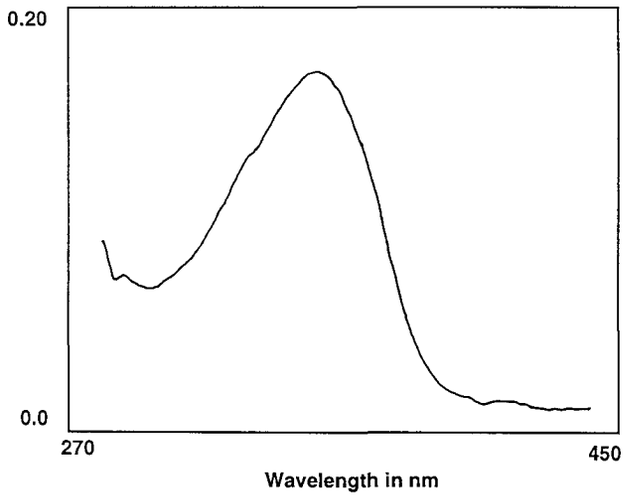

Figure 2 Absorption spectrum for M20 in DMF at ambient temperature

Table 1 Absorbance in DMF at ambient temperature

Compound	λ_{max} (nm)	ε (M cm^{-1})
Model	316	60 000
M20	348	46 000
M50	350	45 000

Excitation and emission spectra

Figure 3 depicts the excitation and emission spectra for M50 in DMF. The model compound and M20 have nearly identical characteristics, except that the features for the polymers are red-shifted from those of the model compound. In each case the excitation spectra closely resembled those for absorptions, having broad bands centred between 320 and 370 nm. The emission shows a very broad band centred around 500 $\pm$ 30 nm. The quantum yields for fluorescence, Q, are larger for the polymers than for the model compound, as shown in *Table 2*.

Aromatic and heteroaromatic nuclei cannot be coplanar in the ground state, S^0, due to large steric repulsions between *ortho*-hydrogen centres. In poly(phenylene) type compounds, however, high degrees of coplanarity are expected in the excited state, S^1. Studies

Table 2 Fluorescence in DMF at ambient temperature

Compound	λ_{ex} (nm)	λ_{em} (nm)	Q^a
Model	325	478	0.0033
M20	348	485	0.0078
M50	365	485	0.0088

[a] The uncertainty in Q is about $\pm$10%

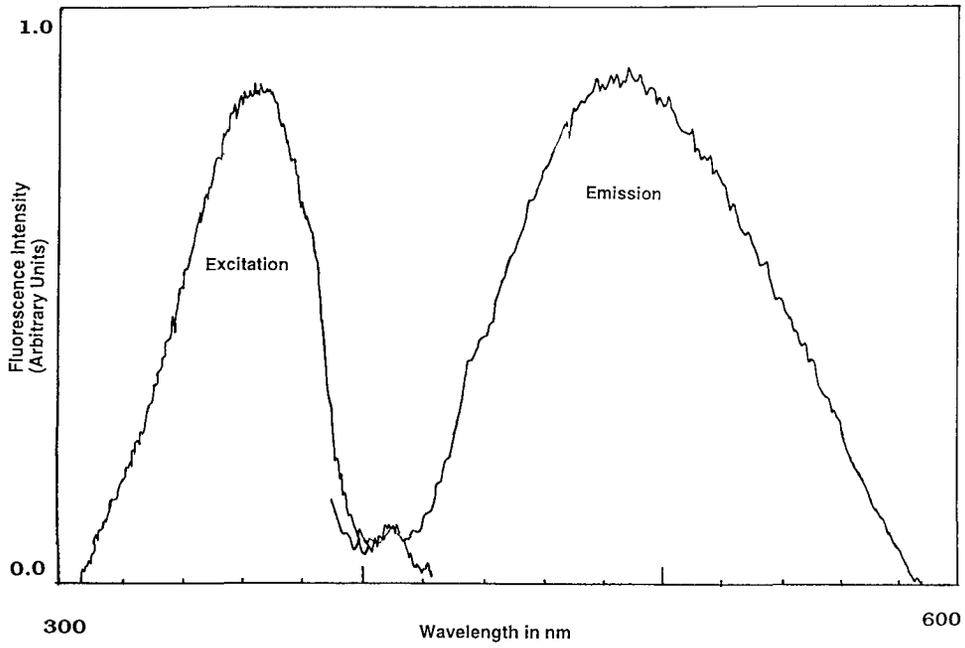

Figure 3 Excitation and emission spectra for M50 in DMF at ambient temperature

Table 3 Calculated R_0 and k_T for the model compound in DMF

κ^2	R_0 (nm)	k_T (s^{-1})
0	0	0
2/3	6.2	5×10^{11}
1	7.0	6×10^{11}
4	11.0	9×10^{11}

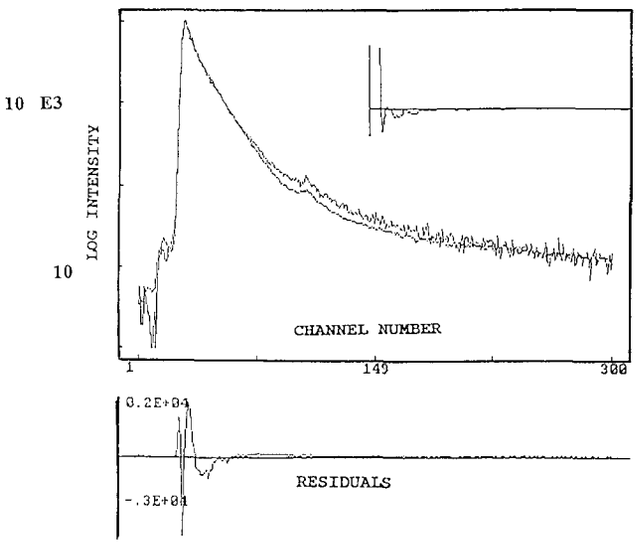

Figure 4 Decay of the fluorescence for M20 in DMF at 25°C

on *p*-terphenyl show a non-coplanar S^0 state[10,11], yet the excited singlet state has been shown to be coplanar[12–14]. Increased resonance interactions in the excited states of these compounds lead to the addition of π character to the coannular bonds, compelling them to become more coplanar[15]. Increases in fluorescence intensity have been observed as a function of increasing planarity of the S^1 state[16]. The response of the polymers and model compound in this study can be rationalized by reference to these findings. The polymers can form more extensive conjugated ring systems in the excited S^1 state than can the model compound, which only has two chromophoric centres. As a result of the increased π character in the polymers, the transition spacings become closer in energy and a red shift of emission is observed relative to the model compound.

Examination of the spectra also reveals a significant overlap between the excitation and emission bands in all of the species. Strong overlaps of the ground and excited electronic states contribute to the probability of nonradiative energy transfer. High rates of intramolecular transfer have been reported in similar bichromophoric phenyl-substituted pyridinium salts[6]. The rate and efficiency of intramolecular transfer for the model compound were calculated using[4]

$$k_T=\frac{8.8\times10^{-25}\kappa^2 Q_d}{n^4\tau_d R^6}\int_0^\infty F_d(\nu)\varepsilon_a(\nu)\frac{d\nu}{\nu^4} \quad (4)$$

$$E=\frac{1}{1+(R/R_0)^6} \quad (5)$$

where the Förster radius, R_0, is defined as the distance between the chromophores at which the efficiency, E, for transfer is 50%. It depends upon the overlap of emission from the donor and excitation of the acceptor, the quantum yield of the donor, the extinction coefficient for the acceptor, refractive index of the solvent, and an orientation factor, κ^2, which is dependent on the relative alignment of the transition dipole of donor and acceptor. The rate of transfer, k_T, includes the donor lifetime, τ_d, and separation between the chromophores, R.

Table 3 lists the calculated results for transfer rate and Förster radius for the model compound, assuming different values for the orientation factor, κ^2, over the physically significant range. It is clear that transfer between chromophoric units along the backbone of the chain is highly probable unless κ^2 is very close to 0. Also, as will be shown below, the calculated values of k_T are comparable in magnitude to the computed rates of the crossing of the barrier at $0\pm90°$ unless κ^2 is very small.

Fluorescence lifetimes

Figure 4 presents the decay curves for M20 as a dilute solution in DMF. The decays of the model compound and M20 were fitted to either a single exponential or a sum of two exponentials.

$$I(t)=\alpha\exp(-t/\tau) \quad (6)$$

$$I(t)=\alpha_1\exp(-t/\tau_1)+\alpha_2\exp(-t/\tau_2) \quad (7)$$

The results are reported in *Table 4*. The model compound in the glass had lifetimes in the range 2–5 ns. In solution, however, the decay for the model compound simplified to a single exponential, and the lifetime decreased by an order of magnitude. The description of the decay for the polymers, in contrast, requires the sum of at least two exponentials. Neither lifetime is larger than 1 ns.

The fluorescence lifetimes are significantly shorter than the correlation times expected for the rotational diffusion of M20 and M50 as rigid rods. For example, a rod of 100 nm length in a solvent of the same viscosity as DMF is expected to have a slow mode (rotation about the short axis) and a fast mode (rotation about the long axis) of the order of $\sim10^{-6}$ s and $\sim10^{-11}\,s^{-1}$, respectively[17]. The molecular weight of M20 implies a length of 120 nm. Therefore the estimated correlation times for rotational diffusion of M20 are much longer than the fluorescence lifetimes.

Anisotropy of the fluorescence

The model compound was used to determine the relative orientations of the transition moments in the repeat unit by taking measurements in the vitrified glassy state. The excitation polarization spectrum for the model compound in a PMMA glass disc, as a function of the wavelength of excitation, is shown in *Figure 5*. The values of the anisotropy are negative across the spectrum. This result denotes non-colinear transition dipoles. The relative angle, θ, between the absorption and emission

Table 4 Fluorescence lifetimes[a]

Compound	Solvent	τ_1 (ns)	τ_2 (ns)	$f_1=1-f_2$
Model	PMMA	2.0	4.9	0.44
Model	DMF	0.12		1
Model	DMF	0.12	6.7	0.99
M20	DMF	0.95	0.58	0.70
M50	DMF	0.57	0.04	0.02

[a] $f_i=\alpha_i\tau_i(\alpha_1\tau_1+\alpha_2\tau_2)^{-1}$

dipoles of the chromophore was calculated from the anisotropy, r_0, in the glass using the relationship[4]:

$$r_0 = \frac{3\cos^2\theta - 1}{5} \tag{8}$$

The values for θ are in the range $80 \pm 10°$. Interpretation of this result must recognize that the model compound contains two chromophores. The drawing at the bottom of *Figure 1* suggests parallel or colinear transition moments for identical electronic transitions in the two chromophores, because both pyridine rings are in the plane of the paper. Different orientations may exist in the real model compound, due to torsion about the bonds between the rings. The actual angles between the planes of the two pyridine rings, ψ, will be:

$$\psi = \Delta\phi_{nc} + \Delta\phi_{mec2} + \Delta\phi_{nc} \tag{9}$$

where each $\Delta\phi$ can assume two values, as shown in *Figure 6*. Assuming no correlations in the signs, the values of ψ should be $\pm 14°$, $\pm 44°$, $\pm 78°$, in the ratio 1:2:1. If the rate of energy transfer between the two chromophores in the model compound was much faster than the rate of emission, this dispersion for ψ might reduce r_0 to a value as small as 0.2. It could not, however, produce $r_0 < 0$.

We conclude that the transition dipoles for absorption and emission are not colinear in a particular chromophore. The non-linearity of these two transition dipoles might arise from a change in conformation of the chromophore upon excitation, as occurs in *p*-terphenyl[10–13]. This conformational change would require a rotation of about 45–60° about bonds from the heteroaromatic ring to the aromatic rings.

The depolarization of emission was also measured for

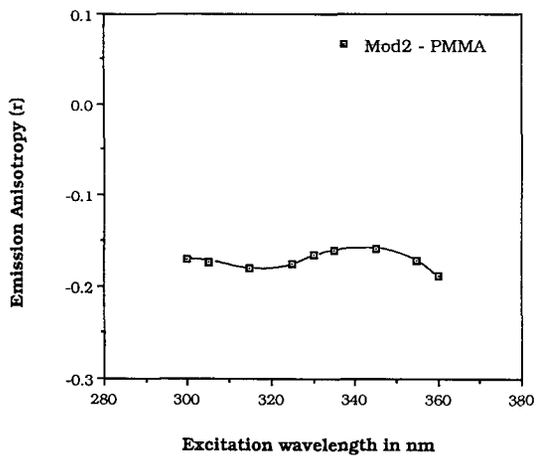

Figure 5 Excitation polarization spectra for the model compound in a vitrified PMMA glass matrix at 25°C. Data are restricted to the range where the excitation is no less than one half of the maximum

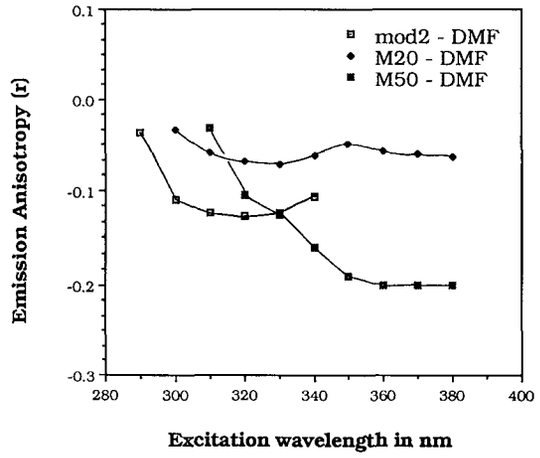

Figure 7 Excitation polarization spectra for the model compound (□) and the polymers [(◆) M20, (■) M50] in dilute DMF solutions at 25°C. Data are restricted to the range where the excitation is no less than one half of the maximum

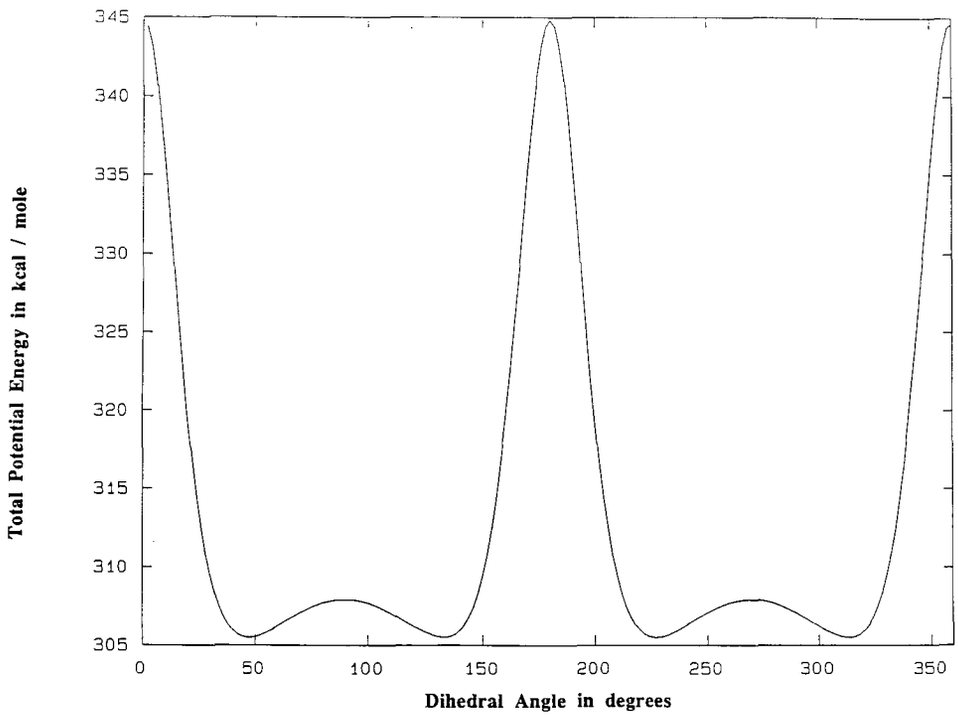

Figure 6 Potential energy *versus* dihedral ϕ_{pcc}. Similar results for ϕ_{nc} place the minima at 61° from planarity, and for ϕ_{mec1} and ϕ_{mec2} the minima are 44° from planarity

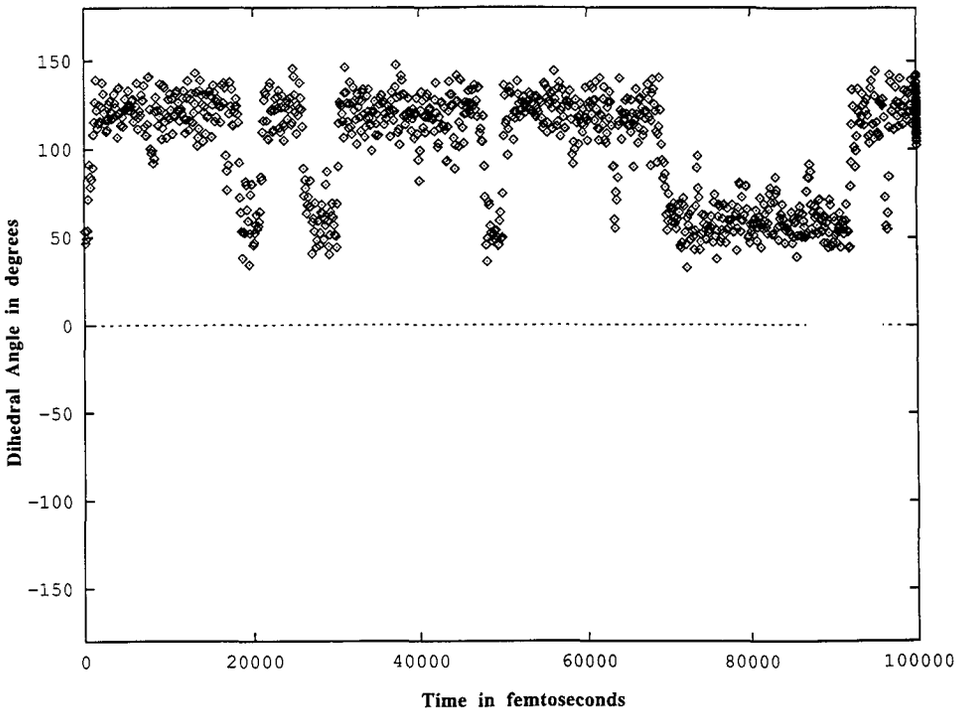

Figure 8 Trajectory for ϕ_{pcc}

dilute solutions of the model compound and polymers in DMF. *Figure 7* depicts the anisotropy as a function of excitation wavelength for the model compound, M20 and M50. A decrease in the absolute value of the anisotropy was observed for the model compound and M20 compared with the results for the model compound in the glass, and this decrease is stronger for M20 than for the model compound. The situation is less clear for M50 because r varies more strongly with the wavelength of excitation.

Conformations of minimum energy

The potential energy for the dimer was examined as functions of the dihedral angles defined in *Figure 1*. The conformations preferred by these bonds, as determined by minimization of pairwise interdependent rotations for each combination of neighbouring bonds, are ~ 44–$61°$ from planarity, as was shown in *Figure 6*. Inclusion or exclusion of partial charges and electrostatic potentials perturbed neither the positions of the minima nor the barrier heights appreciably. Positions for the minima are in good agreement with recent X-ray crystallographic work on similar *ortho*-substituted *para*-phenylene oligomers, which reported values for ϕ_{nc} and ϕ_{pcc} of 51.2° and 55.7°, respectively[18]. The barrier height at $0 \pm 90°$ (2.3 kcal mol^{-1}) agrees well with *ab initio* and semi-empirical results for biphenyl[19]. On the other hand, the barrier heights at 0° and 180° are overestimated in *Figure 6*, based on comparison with the much smaller result of 1–2 kcal mol^{-1} measured for biphenyl[20]. The discrepancy for the larger barrier is likely due to the additional 2- and 6-phenyl substituents, and to the restriction of the minimization procedure to pairwise rotations. In fact, all three rings (2-, 6- and *N*-) are involved in a cooperative transition from one degenerate minimum to another, as can be seen in the molecular dynamics trajectory.

Time dependence of the local conformation

Figure 8 depicts the time dependence of ϕ_{pcc} over 0.1 ns. It shows several transitions over the smaller barrier, at $\phi_{pcc} = 0 \pm 90°$, but no crossings on this time scale over the larger barrier at 0° and 180°. Very similar results are obtained for the time dependence of ϕ_{nc}. More extensive motion occurs at the C–C bonds in the main chain, as shown in *Figure 9*. Here there are transitions across ϕ_{mcc1} of 0° and 180°. Transitions across this barrier are facilitated by in-plane and out-of-plane bending of the *ortho*-hydrogens.

The rates for crossing of the barrier at $\pm 90°$ can be estimated at $\sim 1 \times 10^{11}$ s^{-1} for ϕ_{nc} and ϕ_{pcc}, and $\sim 3 \times 10^{11}$ s^{-1} for the C–C bonds in the main chain. The latter bonds have a rate in the range of 2–3×10^{11} s^{-1} for crossing the barrier at 0° and 180°. These rates are of importance for the depolarization of the fluorescence.

CONCLUSIONS

Polymers and a model compound of a new family of poly(pyridinium salt)s exhibit fluorescence emission. The chromophoric unit is similar to other *ortho*-substituted pyridinium salts, having similar absorbance bands denoting charge transfer complexation of the 2,6- and 4-phenyl substituents with the heteronuclear pyridinium moiety. Molar extinction coefficients and absorption spectra are those expected based on the allowed π–π^* transitions common to similar aromatic ring systems. Fluorescence measurements support the existence of a planar S^1 conformation, as has been reported in other polyphenylene structures. High rates of intramolecular non-radiative energy transfer are expected for these molecules, as calculated from the overlap of excitation and emission bands and the close spacing of chromophoric moieties along the backbone of the polymer. The relative alignment of the transition dipoles for excitation and

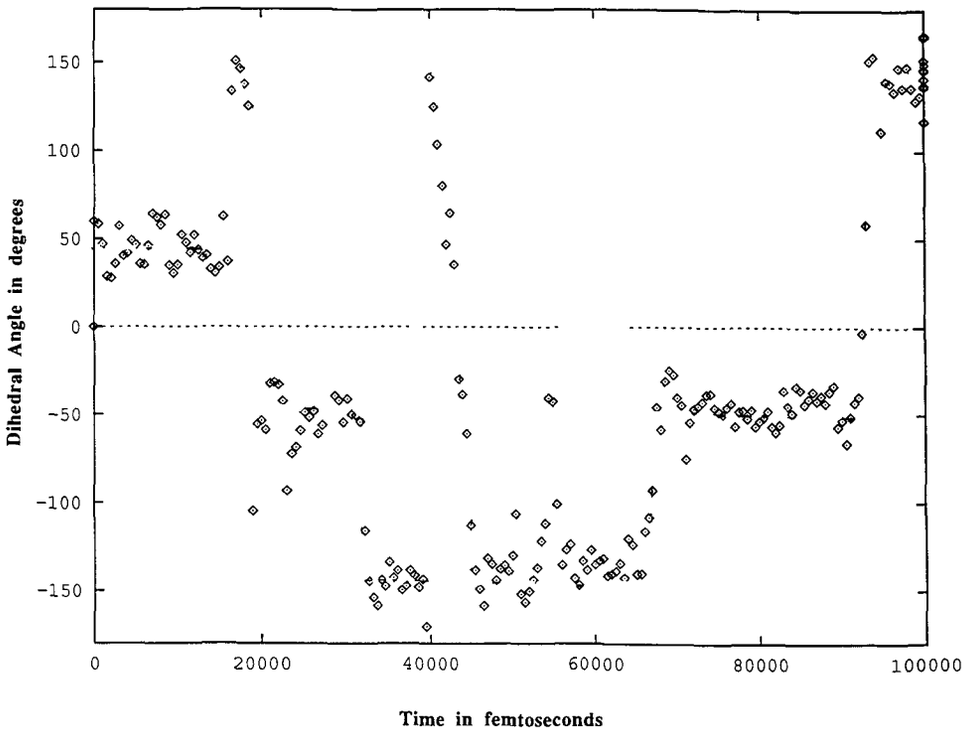

Figure 9 Trajectory for ϕ_{mec}

emission in the repeat unit was found to be non-colinear from anisotropy measurements in the vitrified glass. Significant changes in the relative orientation of the emission dipoles relative to the dipole for excitation were observed in solution relative to the glassy state. The dominant cause of the depolarization of the polymers in dilute solution is not likely to be due to the rotational diffusion of the molecule as a rigid rod, because the characteristic times expected for this diffusion in DMF are much longer than the fluorescence lifetimes. Three excellent candidates for major contributors to the depolarization are obvious. First, there is the change in conformation of the individual chromophore upon excitation from S^0 to S^1, reflecting the greater preference for coplanarity in S^1. Second, there is the likelihood of migration of the excitation along the chain by a Förster transfer mechanism, with a characteristic time for transfer that is faster than the fluorescence lifetime. Hence the chromophore responsible for emission may be different from the one that was responsible for excitation. Finally, there is the rapid change in the local conformation in the ground state, as revealed in the molecular dynamics trajectories. These changes have a characteristic time that is at least as fast as the fluorescence lifetime. The combination of energy migration and rapid conformational changes in the ground state implies a loss of correlation in the transition moments for excitation and emission.

ACKNOWLEDGEMENTS

This research was supported by National Science Foundation Grant DMR 89-15025. We thank Professor Frank W. Harris for supplying the samples used in this project.

REFERENCES

1 Chuang, C. and Harris, F. W. *Am. Chem. Soc., Div. Polym. Chem. Polym. Prepr.* 1989, **30**, 433
2 Katrinsky, A. and Leahy, D. E. *J. Chem. Soc., Perkin Trans. II* 1985, 171
3 Abdel-Khalik, S. I. and Bird, R. B. *Biopolymers* 1977, **14**, 1915
4 Lakowicz, J. 'Principles of Fluorescence Spectroscopy' Plenum, New York, 1986
5 Mendicuti, F. and Mattice, W. L. *Polym. Bull.* 1989, **22**, 557
6 Melhuish, W. H. *J. Phys. Chem.* 1961, **65**, 229
7 Katrinsky, A., Zakaria, Z., Lunt, E., Jones, P. and Kennard, O. *J. Chem. Soc., Chem. Commun.* 1979, 268
8 Katrinsky, A., Agha, B., de Ville, G. Z., Lunt, E., Knyazhanskii, Y., Tymyanskii, Y. and Pyshchev, A. *Khim. Geterotsikl. Soedin.* 1984, **11**, 1509
9 Marchalin, S., Fahnrich, J., Popl, M. and Kuthan, J. *Collect. Czech. Chem. Commun.* 1986, **51**, 1061
10 LeFevre, R. J., Sundaram, A. and Sundaram, K. M. S. *J. Chem. Soc.* 1963, 3180
11 Barrio, M. C., Barrio, J. R., Walker, G., Novelli, A. and Leonard, N. J. *J. Am. Chem. Soc.* 1973, **95**, 4891
12 Berlman, I. B., Wirth, H. O. and Steingraber, O. J. *J. Phys. Chem.* 1971, **75**, 318
13 Momicchioli, F., Bruni, M. and Barald, I. *J. Phys. Chem.* 1972, **76**, 3983
14 Gershuni, S., Rabinowitz, M., Arganat, I. and Berlman, I. *J. Phys. Chem.* 1980, **84**, 517
15 Jaffe, H. H. and Orchin, M. 'Theory and Applications of UV Spectroscopy' Wiley, New York, 1962
16 Berlman, I. B. *J. Phys. Chem.* 1970, **74**, 3085
17 Nishijima, J. *Macromol. Sci. Phys.* 1978, **8**, 407
18 Baker, K. N., Fratini, A. V. and Adams, W. W. *Polymer* 1990, **31**, 1623
19 Tsuzuki, S. and Tanabe, K. *J. Phys. Chem.* 1991, **95**, 139
20 Carreira, L. A. and Towns, T. G. *J. Mol. Struct.* 1977, **41**, 1